International Journal of Nanomedicine

Dovepress
open access to scientific and medical research

Open Access Full Text Article

ORIGINAL RESEARCH

Cellular Uptake and Transport Mechanism of 6-Mercaptopurine Nanomedicines for Enhanced Oral Bioavailability

Yaru Zou[1,2], Wei Gao[3], Huizhen Jin[2], Chenmei Mao[2], Yi Zhang[1], Xiaoling Wang[1], Dong Mei[1], Libo Zhao[1,4]

[1]Department of Pharmacy, Beijing Children's Hospital, Capital Medical University, National Center for Children's Health, Beijing, 100045, People's Republic of China; [2]Department of Pharmacy, Children's Hospital of Soochow University, Suzhou, Jiangsu, 215025, People's Republic of China; [3]Department of Pharmaceutical Sciences, College of Pharmacy, Rogel Cancer Center, University of Michigan, Ann Arbor, MI, 48109, USA; [4]Department of Pharmacy, Peking University Third Hospital, Beijing, 100191, People's Republic of China

Correspondence: Dong Mei; Libo Zhao, Email meidong11290926@126.com; libozhao2011@163.com

Background: Nanomedicines have significant advantages in enhancing the oral bioavailability of drugs, but a deeper understanding of the underlying mechanisms remains to be interpreted. Hence, the present study aims to explain the uptake and trafficking mechanism for 6-MP nanomedicines we previously constructed.

Methods: 6-MP loaded poly(lactide-co-glycolide) (PLGA) nanomedicines (6-MPNs) were prepared by the multiple emulsion method. The transcytosis mechanism of 6-MPNs was investigated in Caco-2 cells, Caco-2 monolayers, follicle associated epithelium (FAE) monolayers and rats, including transmembrane pathway, intracellular trafficking, paracellular transport and the involvement of transporter.

Results: Pharmacokinetics in rats showed that the area under the curve (AUC) of 6-MP in the 6-MPNs group (147.3 ± 42.89 μg/L·h) was significantly higher than that in the 6-MP suspensions (6-MPCs) group (70.31 ± 18.24 μg/L·h). The uptake of 6-MPNs in Caco-2 cells was time-, concentration- and energy-dependent. The endocytosis of intact 6-MPNs was mediated mainly through caveolae/lipid raft, caveolin and micropinocytosis. The intracellular trafficking of 6-MPNs was affected by endoplasmic reticulum (ER)-Golgi complexes, late endosome-lysosome and microtubules. The multidrug resistance associated protein 4 (MRP4) transporter-mediated transport of free 6-MP played a vital role on the transmembrane of 6-MPNs. The trafficking of 6-MPNs from the apical (AP) side to the basolateral (BL) side in Caco-2 monolayers was obviously improved. Besides, 6-MPNs affected the distribution and expression of zona occludens-1 (ZO-1). The transport of 6-MPNs in FAE monolayers was concentration- and energy-dependent, while reaching saturation over time. 6-MPNs improved the absorption of the intestinal Peyer's patches (PPs) in rats.

Conclusion: 6-MPNs improve the oral bioavailability through multiple pathways, including active transport, paracellular transport, lymphatic delivery and MRP4 transporter. The findings of current study may shed light on the cellular uptake and transcellular trafficking mechanism of oral nanomedicines.

Keywords: nanomedicines, oral bioavailability, cellular uptake, transport mechanism

Introduction

6-Mercaptopurine (6-MP) is one of the most commonly used drugs in clinical practice, which comprises the backbone of oral continuing therapy of childhood acute lymphocytic leukemia (ALL).[1] However, its low water solubility, short half-life, poor bioavailability and serious side effects have limited its clinical efficacy.[2] Thus, it is necessary to develop appropriate formulations to overcome these defects.

In recent years, researchers have employed different effective methods to improve the delivery of 6-MP.[3–5] The application of nanotechniques in oral drug delivery shows unique advantages for increasing the bioavailability of poorly water-soluble drugs. In our previous study, we constructed the 6-MP loaded nanomedicines (6-MPNs) with poly(lactide-

Received: 25 October 2022
Accepted: 22 December 2022
Published: 5 January 2023

co-glycolide) (PLGA) through the modified double emulsion method. It has been confirmed that 6-MPNs enhanced the oral bioavailability of 6-MP because of its increased duodenal absorption.[6] Nevertheless, 6-MPNs need to overcome the intestinal epithelial cell barriers before being absorbed into the blood circulation. How nanomedicines promote transmembrane absorption and transport remains to be further studied.

A recent study demonstrated that nanomedicines entered the cells through the following different pathways: (1) Traditional opinions suggested that the drugs in nanomedicines were transmitted via intestine barrier in the molecular form.[7] (2) Some other perspectives demonstrated that nanomedicines might alter the traditional absorption pathways of drugs. In particular, nanomedicines were able to trigger endocytosis, thereby enhancing the capability of drugs to cross the intestinal epithelial cell membrane.[8] (3) The microfold cells (M cells) in the intestinal Peyer's patches (PPs) constitute a natural epithelial barrier together with normal intestinal epithelial cells. Orally administered nanomedicines were taken up by M cells when the particle size is less than 200 nm, which could increase the targeted lymphatic delivery of drugs.[9] (4) The epithelial intercellular tight junctions (TJs) also constitute a natural physiological barrier and affect the permeability of drugs. Yu SH et al[10] reported that nanomedicines might affect the tight junctions and promote the paracellular pathway of drugs. (5) In addition, the drugs are translocated into and out of cells by drug transporters, which influence the drug accumulation within cells.[11] In consideration of above aspects, they all might play important roles in affecting bioavailability. However, their detailed functional mechanisms in the absorption process of nanomedicines are seldom mentioned. Moreover, the absorption mechanisms of different nanomedicines are not exactly the same.

It is known that 6-MP is a biopharmaceutic classification system (BCS) class II drug with the characteristics of low solubility and high permeability, which limits its absorption.[12] 6-MPNs ameliorated the poor water solubility of 6-MP, potentially allowing more free drugs to enter intestinal cells. We also speculated that 6-MPNs might enter the cells via different endocytic pathways and that there exist multiple pathways for intracellular trafficking after internalization.[13] It has been reported that 6-MP and its metabolites are transferred by a multidrug resistance-associated protein 4 (MRP4) transporter. MRP4 polymorphisms are related to 6-MP dose tolerance during maintenance therapy.[14,15] We assumed that 6-MPNs might affect the direct binding of the drugs to MRP4, thereby influencing the efflux of 6-MP.

In order to explain the absorption and transport mechanism of 6-MPNs completely and deeply, we investigated the processes of intestinal uptake and the transport characteristics of 6-MPNs utilizing three cell models, including Caco-2 cells, polarized Caco-2 monolayers and follicle-associated epithelium (FAE) monolayers. Uptake experiments of 6-MPNs through the PPs in the intestines of rats were performed to evaluate the absorption mechanisms of 6-MPNs in vivo.

Materials and Methods

Materials

6-Mercaptopurine (assay purity 98.0%) was provided by Toronto Research Chemicals Inc (Toronto, Canada). Poly (lactide-co-glycolide) (PLGA), poly(vinyl alcohol) (PVA), dichloromethane (DCM), ethyl acetate (EA), dimethyl sulfoxide (DMSO), genistein, ethyl-isopropyl-amiloride (EIPA), chlorpromazine hydrochloride (CPZ), cytochalasin D (Cyt D) and indomethacin were obtained from Sigma-Aldrich Co., Ltd (St. Louis, MO, USA). Pluronic F68 was purchased from Yuan Ye Bio-Technology Co., Ltd (Shanghai, China). Methyl-beta-cyclodextrin (MβCD) was provided by J&K Scientific Ltd. (Beijing, China). Brefeldin A (BFA), nocodazole and dynasore were obtained from Cayman Chemical Company (Ann Arbor, MI, USA). Monensin was bought from MP Biomedicals (Santa Ana, CA, USA). Bafilomycin A1 (Baf-A1) was purchased from Aladdin Bio-Chem Technology Co., Ltd (Shanghai, China).

The primary antibody for ZO-1 was obtained from Abcam Trading Company Ltd (Shanghai, China). Various secondary antibodies were purchased from Invitrogen (Carlsbad, CA, USA). The Cell Counting Kit-8 (CCK-8) was purchased from Dojindo (Shanghai, China). Alkaline Phosphatase (ALP) assay kit was bought from the Nanjing Jiancheng Bioengineering Institute (Nanjing, China). Bicinchoninic acid (BCA) protein assay kit was provided by BestBio Biological Reagent Co., Ltd (Shanghai, China). Nonessential amino acid (NEAA) and fetal bovine serum (FBS) were obtained from Gibco Invitrogen Co. (Carlsbad, USA). Triton X-100, goat serum and 4% paraformaldehyde were obtained from Solarbio Technology Co., Ltd (Beijing, China). Radio-immunoprecipitation assay (RIPA) lysis buffer and phenyl methyl sulfonyl fluoride (PMSF) were purchased from BioDee Biotechnology Co., Ltd (Beijing, China).

Transwell chambers (3 μm pore size, 12 wells) were purchased from Corning Costar, Inc. (Cambridge, MA, USA). All other reagents were analytical or chromatography grade.

Cell Lines and Animals

The Caco-2 cell line and the Raji cell line were gained from the Type Culture Collection of Chinese Academy of Sciences (Shanghai, China). Sprague-Dawley (SD) rats weighing about 250 g were obtained from Beijing Vital River Laboratory Animal Technology (Beijing, China). The SD rats were divided into 6-MP suspensions (6-MPCs) group and 6-MPNs group. SD rats were housed under standard animal feeding conditions with ad libitum access to water and food. All care and handling of animals were strictly in accordance with the Animal Welfare Act and the Guide for the Care and Use of Laboratory Animals protocols. Animal studies were approved by the Animal Ethics Committee of Capital Medical University (Approval Number: AEEI-2020-072).

Preparation and Characteristics of 6-MPNs

Preparation of 6-MPNs and 6-MP Suspensions

6-MPNs were prepared by a modified double-emulsion solvent evaporation method.[6] Briefly, 6-MP and poly(vinyl alcohol) (PVA) were dissolved in ammonia water to form the aqueous phase. The drug-containing solution was added dropwise into the ethyl acetate containing PLGA while stirring to achieve w/o emulsion. The primary emulsion was sonicated and then poured into the aqueous phase containing 1% w/v Pluronic F68. The mixed emulsion was sonicated again to obtain the w/o/w emulsion. Finally, we removed the organic solvent in the double emulsion by rotary evaporation. The prepared nanomedicines were centrifuged, washed and lyophilized using mannitol as a cryoprotectant to formulate 6-MPNs. We added 6-MP into 0.5% (w/v) sodium carboxymethyl cellulose solution (CMC-Na) to prepare 6-MPCs.

Physicochemical Properties and Morphology Characterization

The particle size and zeta potential of 6-MPNs were measured using dynamic laser scattering (DLS, Malvern Instruments Ltd., Malvern, UK). The morphologies of the 6-MPNs were characterized by Transmission Electron Microscope (TEM, JOEL, JEM 2100). 6-MPNs were dispersed in different media including DMEM and DMEM with 10% FBS. The physicochemical stability was assessed by measuring their particle size at 37°C for different incubation times.

In vitro Release of 6-MPNs

The in vitro release of 6-MPNs was analyzed by the dialysis method.[16] 6-MPNs or 6-MPCs (2 mg/mL) were added into dialysis bags, then dialyzed against PBS (pH 7.4) containing 0.02% (v/v) tween 20 at 37 ± 2°C. At predetermined intervals, we withdrew PBS (1.0 mL) and refilled it with equal amounts of fresh PBS. The samples were centrifuged (12,000 g, 15 min) to collect the supernatants.

The drug content in 6-MPNs was quantified by HPLC (Shimadzu, Kyoto, Japan) performed on Diamonsil C_{18} column with mobile phase of phosphate buffer (pH = 3.31)-acetonitrile (75%: 25%, v/v) at flow rate of 1.0 mL/min. The column oven temperature was set at 40°C, and the UV detection wavelength was 325 nm.[17]

In vivo Pharmacokinetics in SD Rats

The SD rats were orally administered 6-MPCs or 6-MPNs at a dose of 15.75 mg/kg. At various time points after administration, blood samples were collected from the orbit of the rats and centrifuged at 5000 g for 10 min at 4°C. The plasma samples were added with methanol to precipitate protein and then centrifuged at 16,000 g for 10 min.[18] The concentration of 6-MP in the supernatants was determined by HPLC-MS/MS.

MS analysis was performed using an API 5500 triple-quadrupole mass spectrometer (Applied Biosystems-Sciex, Toronto, Canada). The mobile phase consisted of methanol containing 0.5% v/v formic acid and water. Chromatographic separation was achieved with gradient elution on an Atlantis T3 column (2.1 mm × 100 mm, 5 μm) with gradient elution. We employed that a flow rate was 0.4 mL/min, a sample injection volume was 3 μL and a run time was 5 min. The column oven and autosampler were set at 37°C and 10°C, respectively. Multiple reaction monitoring transition was

performed for quantitation at m/z 153.0 > 118.9 for 6-MP.[19] The pharmacokinetic parameters were calculated by the standard noncompartmental analysis (NCA) in Phoenix WinNonlin version 7.0 (Certara, Princeton, NJ).

The Uptake and Transport Mechanism of 6-MPNs in Caco-2 Cells

Cytotoxicity Study

The viability of Caco-2 cells was analyzed by the CCK-8 method.[20] Caco-2 cells were seeded in 96-well culture plates at a density of 1×10^5 cells/mL. When Caco-2 cell culture reached about 90% confluency, the cells were intervened with 6-MPNs or 6-MPCs at different concentrations for 4 h. The negative control group was treated with DMEM media without drugs. After incubation, the media were discarded and the cells were subsequently treated with 100 μL fresh serum-free DMEM containing 10 μL CCK-8 solution for another 1 h at 37°C. The absorbance was measured at 450 nm using a Spectra MAX 190 microplate reader.

Determination of Total Protein and Drug Content in Caco-2 Cells

The total protein contents of Caco-2 cells were determined by BCA assay.[21] When Caco-2 cells were incubated with the drugs, we discarded the drug-containing media and washed the cell surface three times with PBS. Caco-2 cells were extracted with RIPA lysis buffer containing 1% PMSF for 0.5 h on ice. The lysed cell suspensions were transferred into Eppendorf (EP) tubes and vortexed at 10 min intervals followed by centrifugation at 12,000 g for 15 min. The supernatants were collected, and the total proteins were determined by BCA protein assay kit. 100 μL of cell lysates were mixed with 300 μL of methanol to promote protein precipitation. Then, the samples were centrifuged at a speed of 14,000 g for 10 min, and the drugs in supernatants were detected by HPLC.

Effects of Different Factors on Endocytosis

To study the time dependence of endocytosis, Caco-2 cells were seeded in 6-well plates in a density of 1×10^5 cells/mL. After the cell fusion degree reaching approximately 90%, the cells were treated with 100 μM of 6-MPNs or 6-MPCs for 0.5 h, 1 h, 2 h, 3 h and 4 h. Similarly, the cultured Caco-2 cells were incubated with 6-MPNs or 6-MPCs at different concentrations (50 μM, 100 μM, 200 μM and 400 μM) for 2 h. Separately, for energy dependence investigation of endocytosis, Caco-2 cells were cultured as previously described and pre-incubated at 4°C or 37°C for 1 h. Then, 100 μM 6-MPNs or 6-MPCs were added, respectively, and cultured at 4°C or 37°C for 2 h.[22]

After incubation, drug-containing media were discarded and pre-chilled PBS buffer were added to complete the Caco-2 cellular uptake. The cells were lysed by RIPA lysis buffer containing 1% PMSF at 4°C. The total protein contents of cells lysates were determined by the BCA assay, and the 6-MP in lysis solution was examined by HPLC as previously described. All data of concentrations were normalized to the total protein contents per well.

Endocytosis and Trafficking Mechanism Analysis

The endocytic pathways and intracellular trafficking mechanism of 6-MPNs were explored using different inhibitors with endocytosis/transport functions or signal transduction pathways (details in Supplementary Materials). [23] Caco-2 cells were seeded in 12-well plates at a density of 1×10^5 cells/mL. After attaining 90% confluency, the cells were pre-incubated with different inhibitors for 0.5 h, respectively. The media were discarded, and the cells were washed three times with PBS. Then, 100 μM 6-MPNs or 6-MPCs were co-incubated with different endocytosis inhibitors containing MβCD, Genistein, EIPA, Cyt D, CPZ and Dynasore at 37°C for 0.5 h. Similarly, 200 μM 6-MPNs or 6-MPCs with different intracellular trafficking inhibitors (BFA, Monensin, Baf-A1 and Nocodazole) were added and incubated at 37°C for 2 h. Concentrations of inhibitors were the same as that of pre-incubation. The intracellular 6-MP contents were measured according to the HPLC method described above.

The Effect of MRP4 Transporter on the Transport of 6-MPNs

Indomethacin is an inhibitor of MRP4 transporter. It is used to study the effect of MRP4 transporter on 6-MP's uptake.[24] Caco-2 cells were seeded in 6-well plates and cultured to 90% confluency. The cells were preincubated with indomethacin (30 μM) at 37°C for 0.5 h. The media were removed, and the cells were washed 3 times with PBS. Then, 100 μM

6-MPNs or 6-MPCs with indomethacin (30 μM) were cultured with cells for 2 h. The control group was treated without indomethacin. The intracellular 6-MP contents were determined using the HPLC method as described above.

Bidirectional Transport Experiments of 6-MPNs in the Caco-2 Monolayers

Assessment of the Polarization of Caco-2 Monolayers

Caco-2 cells were seeded on the transwell filters and cultured for 21 days to form Caco-2 monolayers (details in Supplementary Materials). [25] The differentiation levels of Caco-2 monolayers were estimated by measuring alkaline phosphatase (ALP) activity. DMEM media were collected from the apical (AP) side and the basolateral (BL) side of the transwell chambers before media changed on days 7, 14 and 21. The ALP activity was determined by ALP activity assay kit, and the ratio of ALP activity on the AP sides to the BL sides was calculated.

Bidirectional Transport Assay of 6-MPNs

Bidirectional transport experiments from the AP sides to the BL sides (AP-BL) and from the BL sides to the AP sides (BL-AP) were performed in Caco-2 monolayers. In the AP-BL direction experiments, 200 μM 6-MPNs or 6-MPCs were added to the AP sides as the supplier phase and 1.5 mL blank PBS was added to the BL sides as acceptor phase. For the BL-AP direction experiments, 1.5 mL 6-MPNs or 6-MPCs media and 0.5 mL blank PBS were added to the BL sides and AP sides, respectively. At a predetermined time (0.5, 1, 1.5 and 2 h), 100 μL aliquots were collected from the acceptor phase. Equal volumes of blank PBS were supplemented with each withdrawal. The samples were centrifuged at 15,000 g for 15 min, and the concentrations of 6-MP in the supernatants were analyzed by HPLC to calculate the apparent permeability coefficient (Papp) and efflux ratio (ER).[26]

We also investigated the effect of MRP4 transporter on the bidirectional transport of 6-MPNs. The Caco-2 monolayers were preincubated with indomethacin for 0.5 h at 37°C to inhibit MRP4 transporter. After that, 6-MPNs or 6-MPCs containing 30 μM indomethacin were added to the AP sides or the BL sides as the supplier compartments. Three transwell inserts were used for each treatment in parallel. Other processes were the same as described above.

The Effect of 6-MPNs on Tight Junction Protein (ZO-1) Expression

Immunofluorescence Staining

The expression of tight junction protein (ZO-1) in Caco-2 monolayers was assessed by immunofluorescence staining.[27] The donor chambers in each transwell were added with 100 μM 6-MPNs or 6-MPCs and the lower chambers were filled with 1.5 mL of PBS, which was then incubated at 37°C for 2 h. The media were discarded, and the cell monolayers were washed three times with PBS. After immobilization with 4% paraformaldehyde for 15 min, the cell monolayers were permeabilized with 0.1% Triton X-100 for 15 min and blocked with 5% goat serum at 37°C for 60 min to eliminate nonspecific staining. The cells were incubated overnight at 4°C with the primary antibody of ZO-1. The next day, the cells were incubated with the secondary antibody at 37°C for 60 min. The cell nuclei were stained with Hoechst for 15 min. The staining was observed by a laser confocal microscope.

Western Blot Analysis

Caco-2 cell monolayers were treated with 6-MPNs or 6-MPCs in the same procedures as described in immunofluorescence staining. The cell suspensions were gently scraped into EP tubes and centrifuged at 6000 g for 5 min at 4°C. The lower cells were lysed on ice for 0.5 h in a RIPA buffer containing 1% PMSF, and the total protein contents were detected using BCA Protein assay kit. The proteins and markers were initially subjected to sodium dodecyl sulfate polyacrylamide gel electrophoresis (SDS-PAGE) in 4% stacking gel at 80 V for 15 min and then separated using SDS-PAGE in 7.5% separating gel at 120 V for 1.5 h. The separated proteins were transferred to polyvinylidene fluoride (PVDF) membranes and blocked with 5% skim milk for 1 h at room temperature. The membranes were incubated with ZO-1 antibody overnight at 4°C followed by secondary antibody in the dark for 1 h. After washing twice with PBST, the signals were analyzed using Odyssey CLx imager (Gene Company Limited). The images were analyzed by Image J. The relative amounts of protein were normalized to tubulin.[27]

Uptake and Transport Mechanism Analysis in the FAE Monolayers

Uptake Characteristics and Transport Mechanism of 6-MPNs

FAE monolayers were grown under transport experimental conditions (details in Supplementary Materials). [28] The transwell chambers were transferred to clean 12-well plates. The different concentrations of 6-MPNs or 6-MPCs were added to the AP insert compartments and incubated at 37°C for 2 h. The upper chambers of FAE monolayers were treated with 200 μM 6-MPNs or 6-MPCs and cultured at 37°C for 0.5 h, 2 h, and 4 h, respectively. The FAE monolayers were pre-incubated for 1 h at 4°C or 37°C, respectively. Then, AP sides of FAE monolayers were added with 200 μM 6-MPNs or 6-MPCs and cultured at the corresponding temperature for 2 h. After incubation, the media in the upper and lower chambers were discarded. The cell monolayers were rinsed three times with cold PBS to complete the uptake and lysed with RIPA Lysis buffer containing 1% PMSF for 0.5 h on ice. The obtained cell suspensions were sonicated and centrifuged at 12,000 g for 15 min. The supernatants were collected and their protein contents were determined by BCA assay. The concentrations of 6-MP in the lysates were determined by HPLC. All concentrations were normalized to the total protein content per well.

The incubation experiments described above were repeated to evaluate the cumulative transport of 6-MPNs in FAE monolayers. At different incubation times (0.5, 1, 1.5, 2 and 4 h), 100 μL samples were taken from the BL sides and supplied with equal volumes of PBS at different times. The concentrations of 6-MP were detected by HPLC.

Comparison of Cumulative Transport in the Caco-2 Monolayers and FAE Monolayers

Caco-2 monolayers and FAE monolayers were cultured according to the methods as previously described. 200 μM 6-MPNs or 6-MPCs were added to the upper chambers of Caco-2 monolayers and FAE cell monolayers and incubated at 37°C for 2 h. Samples were taken from the lower chambers at different times, while equal volumes of PBS were added. The cumulative transport of 6-MPNs and 6-MPCs was calculated in both cell monolayer models.

Absorption of 6-MPNs in the Intestinal Peyer's Patches

Absorption experiments of intestinal Peyer's patches (PPs) were carried out using Sprague-Dawley (SD) rats. The SD rats were administrated with 6-MPNs and 6-MPCs by gavage at a dose of 15.75 mg/kg. After 0.5 h, the rats were sacrificed to take the proximal and distal portions of Peyer's patches and the adjacent Peyer's patch-free intestinal tissues.[29] The removed intestinal tissues were prepared into 10% homogenates, and the concentrations of 6-MP were analyzed by HPLC-MS/MS.

Statistical Analysis

All data were reported as the mean ± SD and the data were analyzed using GraphPad Prism 7.0. Prism software was also used for the unpaired *t*-test and P values <0.05 were considered significant.

Results and Discussion

Preparation and Characterization of 6-MPNs

6-MPNs were successfully constructed by a double emulsion solvent evaporation method. The recently reported nanomedicines are prepared with polymers,[30] metal vector,[31] silica,[32] magnetic materials,[33] etc. Preparations of these nanoparticles require complicated experimental procedures and involve safety concerns caused by crosslinkers, surfactants or organic solvents. However, there are limited reports on the 6-MP-loaded oral nanomedicines. Herein, we developed the 6-MPNs with a relatively simple and safe strategy. The obtained 6-MPNs had the superiority for good physicochemical properties, high encapsulation efficiency and exhibited good practical application prospect.

The morphologies of 6-MPNs were observed by TEM. As indicated in Figure 1A, 6-MPNs were uniform spherical in shape. The particle size determined by DLS was 142.56 ± 1.34 nm, with low polydispersity index (PDI) of 0.135 ± 0.011. The surface charge of 6-MPNs was slightly negative of −1.0 mV. We also evaluated the stability of 6-MPNs in different media. Figure S1 shows that the particle size of 6-MPNs could be maintained in a proper range within 48 h in DMEM media and DMEM with 10% FBS media. The results demonstrated that 6-MPNs had sufficient stability to use in the following cellular uptake and transport experiments because the studies were all less than 48 h long. In General, 6-MPNs had appropriate physicochemical properties and dispersion stability.

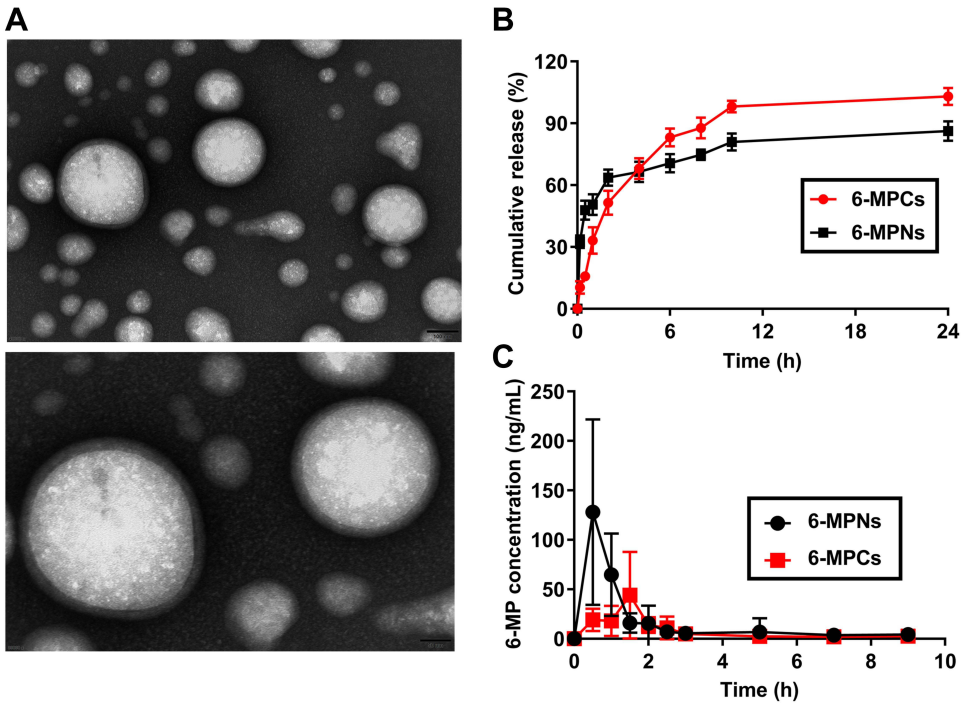

Figure 1 Characterization of 6-MPNs in vitro and in vivo. The morphology of 6-MPNs measured by Transmission Electron Microscope (TEM) (**A**). (**B**) In vitro release of 6-MP from 6-MPNs and 6-MPCs in PBS containing 0.02% Tween 20. (**C**) In vivo plasma concentrations (ng/mL) of 6-MP vs Time (h) profiles after a single oral administration of 6-MPNs or 6-MPCs in SD rats.

Figure 1B shows that 6-MPCs were gradually released to 98.77 ± 2.84% within 10 h. In contrast, the cumulative release of 6-MPNs could achieve 63.64 ± 3.95% in 2 h. The remaining 6-MPNs were released constantly and slowly, finally reaching cumulative release of 86.26 ± 4.70% within 24 h. The results exhibited that 6-MPNs had biphasic release profile with an initial burst release followed by a continuous release. A part of free 6-MP adsorbed on the surfaces of 6-MPNs could be released rapidly, while the drug entrapped within nanomedicines showed a sustained release.[34]

Pharmacokinetic Studies

We further confirmed that 6-MPNs were able to improve the peak concentration (C_{max}) and the area under the curve (AUC) of 6-MP in SD rats.[6] The C_{max} (128.10 ng/mL) and AUC (147.3 ± 42.89 μg/L·h) of 6-MP in the 6-MPNs group were significantly higher than the C_{max} (44.03 ng/mL) and AUC (70.31 ± 18.24 μg/L·h) of 6-MP in the 6-MPCs group (Figure 1C). There was little difference in the half-life (t1/2) of 6-MP between the 6-MPNs and 6-MPCs groups (1.25 ± 0.33 h and 1.27 ± 0.39 h, respectively). The T_{max} of 6-MPNs group (0.81 ± 0.53 h) was shorter than that of 6-MPCs group (1.50 ± 0.56 h). The elimination rate of 6-MPNs group and 6-MPCS group were 42.51 ± 4.00 L/h and 99.12 ± 16.96 L/h, respectively ($P = 0.0058$). The mean residence time (MRT) (5.33 ± 0.20 h) of 6-MP in the 6-MPNs group was significantly higher than the MRT (4.22 ± 0.34 h) of 6-MP in the 6-MPCs group ($P = 0.0129$). One could attribute this to the facts that 6-MPNs exhibited the biphasic release characteristics. The initially rapid release of nanomedicines is conducive to achieving effective blood concentrations, while the sustained release helps extend the retention time in vivo.[34] Nanomedicines could also promote intestinal absorption to increase oral bioavailability.[25] The explanations for the improved oral bioavailability of 6-MPNs were further illustrated in the following analysis.

The Endocytosis Mechanism of 6-MPNs in Caco-2 Cells

Cytotoxicity Analysis of 6-MPNs

We used Caco-2 cells as a cell model to elucidate the endocytosis and transmembrane trafficking mechanism of 6-MPNs. The effect of 6-MPNs on Caco-2 cellular activity was analyzed by CCK-8 assay. We discovered that the survival rate of

Caco-2 cells was greater than 90% after treatment with different concentrations of 6-MPNs and 6-MPCs for 4 h (Figure 2A). The results indicated that 6-MPNs in the concentrations of 5 μM - 400 μM would not significantly affect the activity of Caco-2 cells in subsequent experiments.

Effects of Different Factors on Cellular Uptake

In order to assay the uptake particularity of 6-MPNs, we determined the concentrations of 6-MP in Caco-2 cells at different incubation factors. As displayed in Figure 2B-D, the uptake of 6-MP was gradually enhanced with increase in time, concentration and temperature. Significantly, the cellular uptake of 6-MPNs was greater than that of 6-MPCs at each time point (Figure 2B). The improved uptake of 6-MPNs was the most pronounced at 2 h, so 2 h was chosen as the incubation time for subsequent uptake experiments. The cellular uptake of 6-MPNs was obviously higher than that of 6-MPCs at 100 μM and 200 μM (Figure 2C). However, there was no significant difference in the uptake between 6-MPNs and 6-MPCs at 400 μM, possibly due to the saturated uptake of 6-MPNs. The assimilation of the 6-MPNs was higher than that of 6-MPCs at 4°C and 37°C. The uptake of the 6-MPNs at 4°C was lower than that at 37°C, while there was no significant difference in the uptake of the 6-MPCs at 4°C and 37°C (Figure 2D). The results indicated that the endocytosis of nanomedicines was obviously energy-dependent active transport process, but the uptake of free drugs might be a passive transport process.[35] Overall, 6-MPNs significantly increased the uptake of 6-MP in a time-, concentration- and energy-dependent manner. This might be an explanation that 6-MPNs improved the oral bioavailability of 6-MP.

Endocytosis Mechanism

The endocytosis pathways of 6-MPNs were investigated with various pathway inhibitors. The dosage and function of different inhibitors were displayed in Table S1. Caco-2 cells were incubated with the inhibitors for 4 h to analyze the

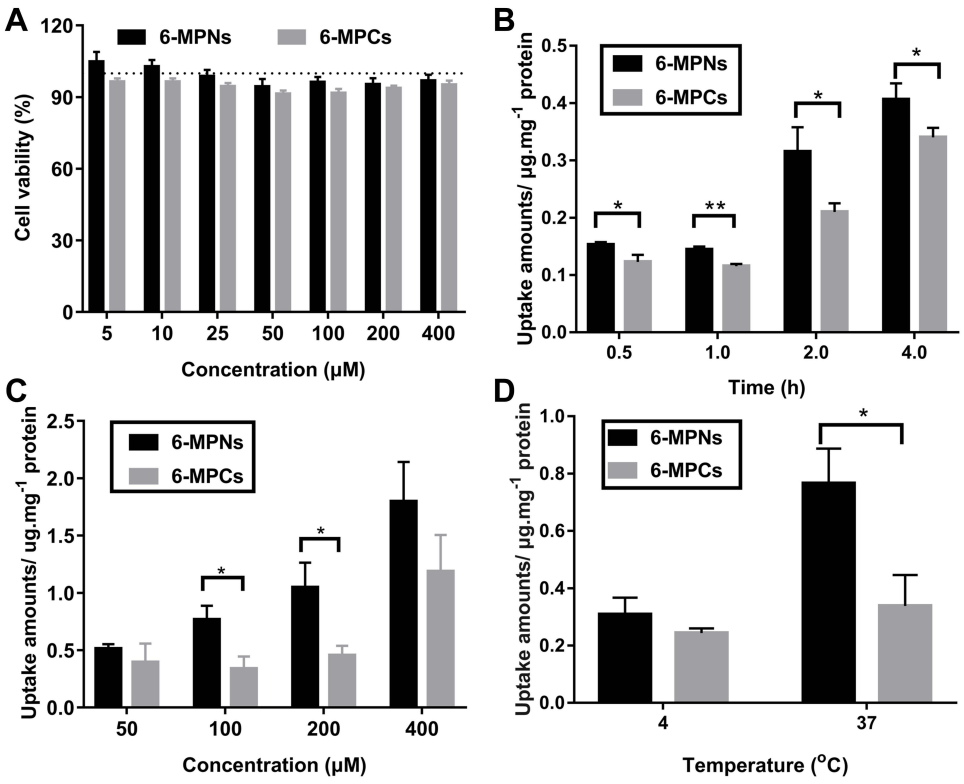

Figure 2 Uptake mechanisms study of 6-MPNs in Caco-2 cells. (**A**) Cytotoxicity analysis of Caco-2 cells incubated with 6-MPNs for 4 h by the Cell Counting Kit-8 (CCK-8) method. (**B**) The effects of time on the uptake of 6-MPNs by Caco-2 cells (**P* value < 0.05, ***P* value < 0.01). (**C**) The effects of concentration on the uptake of 6-MPNs by Caco-2 cells (**P* value < 0.05). (**D**) Analysis of energy dependence of endocytosis of 6-MPNs in Caco-2 cells (**P* value < 0.05).

cytotoxicity. Our results showed that the viability of Caco-2 cells was greater than 90%, indicating that inhibitors did not significantly affect the activity of Caco-2 cells under the experimental conditions (Figure S2).

After intervention with endocytosis inhibitors, 6-MPNs were co-cultured with cells for 0.5 h and intracellular 6-MP was measured with HPLC. As shown in Figure 3A, MβCD, Dynasore and EIPA obviously reduced the internalization of 6-MPNs, while Cyt D, Genistein and CPZ had less influence on the uptake level. MβCD can deplete cholesterol on membranes of cells to inhibit caveolin/lipid raft-dependent endocytosis.[36] Dynasore can block clathrin and caveolin mediated endocytosis pathways.[37] CPZ is an inhibitor of clathrin mediated endocytosis,[38] which had less effect on the uptake of 6-MPNs. The results indicated that the endocytosis of 6-MPNs was related to caveolin and caveolin/lipid raft. Furthermore, EIPA could significantly attenuate the intracellular content of 6-MP by blocking Na^+/H^+ exchange on the cell membrane to inhibit micropinocytosis.[39] Conversely, Cyt D had little effect on endocytosis of 6-MPNs by disrupting actin polymerization to prevent micropinocytosis.[40] The result suggested that the entry of 6-MPNs had poorly correlated with actin-mediated micropinocytosis. Genistein is an inhibitor of tyrosine-specific protein kinases (PTK) and inhibited the expression of caveolin-1 (cav-1).[41] The uptake of 6-MPNs showed no significant difference after intervening with Genistein.

We report cellular endocytosis pathways of nanomedicines including clathrin-dependent endocytosis, caveolin-dependent endocytosis, clathrin- and caveolin-independent endocytosis, phagocytosis and micropinocytosis.[8] Different nanomedicine exhibit different properties and have multiple endocytosis pathways or mechanisms. The cellular internalization pathways of nanomedicines are affected by multifaceted factors. The physicochemical properties of nanomedicines including size, shape, surface charge, composition and architecture, as well as the nature of drug itself, such as molecular weight and solubility, are one of the most important elements.[42] However, there are few researches on the uptake and transport mechanisms of purine analogue nanomedicines. Hence, it is critical to further understand and explore the uptake mechanisms of 6-MPNs. Our findings indicated that the endocytosis of 6-MPNs were mainly mediated by caveolae/lipid raft, caveolin and micropinocytosis, providing the basis for the design of efficient and multifunctional nanomedicines.

Intracellular Trafficking Mechanism

When the uptake is constant, the content of intracellular 6-MP could reflect the exocytosis of 6-MPNs in some extent. We utilized different transport inhibitors to intervene the transport of 6-MPNs, aiming to analyze the classical exocytosis-related intracellular trafficking pathways. Brefeldin A (BFA), Monensin, Bafilomycin A1 (Baf-A1) and Nocodazole all significantly enhanced the content of intracellular 6-MP (Figure 3B). BFA and Monensin are inhibitors of the endoplasmic reticulum-Golgi complex pathway. BFA can specifically inhibit the vesicle trafficking of 6-MPNs from endoplasmic reticulum to Golgi apparatus.[43] Monensin is able to block the transport of 6-MPNs from Golgi to plasma membrane by

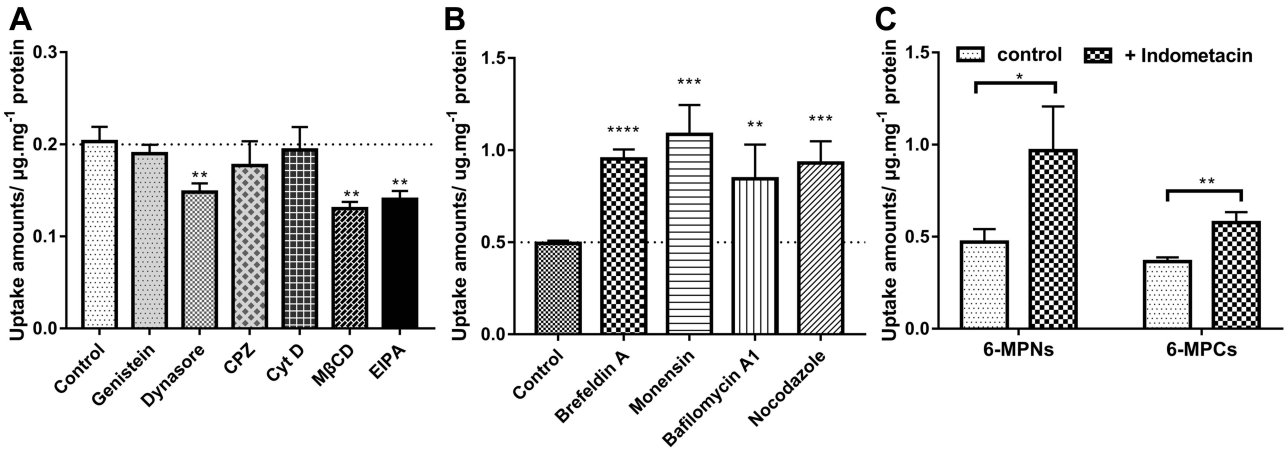

Figure 3 Endocytosis and transport mechanism analysis of 6-MPNs in Caco-2 cells. (**A**) The effect of different endocytosis inhibitors on the internalization of 6-MPNs in Caco-2 cells (**P value < 0.01). (**B**) The effect of different intracellular transport inhibitors on the internalization of 6-MPNs in Caco-2 cells (**P value < 0.01, ***P value < 0.001, ****P value < 0.0001). (**C**) The effect of indomethacin on the transport of 6-MPNs in Caco-2 cells (*P value < 0.05, **P value < 0.01).

disturbing the Golgi apparatus directly.[44] The Golgi apparatus plays an important role in the intracellular trafficking of 6-MPNs.

Furthermore, Baf-A1 is a canonical inhibitor of lysosomal acidification.[45] The increase of intracellular 6-MP content was attributed to late endosome-lysosome pathway mediated by Baf-A1. More 6-MPNs were involved in transmembrane trafficking, rather than directly entering lysosomes for degradation. Nocodazole can disturb the function of microtubules and promote the depolymerization of microtubules.[46] There was a significant increase in intracellular 6-MP content after nocodazole intervention, suggesting that microtubules were significantly associated with the trafficking of 6-MPNs in cells. Hence, 6-MPNs were mainly transmitted from endoplasmic reticulum to Golgi apparatus after entering the cells, and then to the plasma membrane. Lysosomes were involved in the late stage of transport, and microtubules were also involved in 6-MPNs related transport.

After cellular internalization via endocytic pathways, nanomedicines could trigger intracellular trafficking. Membrane vesicles are transported by cell's cytoplasm and intracellular organelles.[47] Similar to nanomedicine cellular uptake, the intracellular trafficking patterns are also mainly dependent on the properties of nanomedicine and the drug itself. Our findings revealed that the intracellular trafficking of 6-MPNs was affected by endoplasmic reticulum (ER)-Golgi complexes, late endosome-lysosome and microtubules. A further profound understanding of 6-MPNs' cellular uptake and trafficking would provide valuable resources for the development of purine analogue nanomedicines.

The Effect of MRP4 Transporter on the Transport of 6-MPNs

Multi-drug resistance-associated protein 4 (MRP4) transporter is an organic anion transporter that transports nucleotide analogs.[48] MRR4 transporter expressed in gut of human and rats and also in the Caco-2 cells.[49,50] We selected indomethacin as the inhibitor of MRP4 transporter to evaluate the effect of MRP4 transporter on the delivery of 6-MPNs.[51] As shown in Figure 3C, we discovered that the intracellular accumulation of 6-MP increased when the function of MRP4 transporter was attenuated by indomethacin. It has been reported that 6-MP was the substrates of the MRP4 transporter, and the efflux of 6-MP was increased in 6-MP resistant cells, in which MRP4 transporter was upregulated.[14] Thus, the impeded cellular efflux of 6-MP leads to the intracellular accumulation of 6-MP after the function of MRP4 transporter was attenuated. The intracellular accumulation of 6-MPNs was more than 6-MPCs after incubated with Caco-2 cells in the presence of indomethacin, suggesting that MRP4 transporter had a significant influence on the trafficking of 6-MPNs. A part of free 6-MP was gradually released from 6-MPNs, possibly due to the increased uptake of 6-MPNs after incubation for 2 h. Overall, intracellular 6-MP for 6-MPNs might originate from passive diffusion, transporter mediated molecular delivery and nanoparticles triggered vesicle transport.[35]

Bidirectional Transport Analysis of 6-MPNs on a Caco-2 Monolayer

Polarity Assessment of Caco-2 Monolayer

Alkaline phosphatase (ALP) is a marker enzyme of brush border cells in the small intestine, and ALP activity is an important indicator for Caco-2 monolayer differentiation.[52] Table S2, showed the ratio of ALP activity of AP side and BL side in Caco−2 monolayer at different times. The ratio of ALP activity progressively increased over time. The value was significantly higher on day 21 (5.36 ± 0.24) than day 9 (3.53 ± 0.46) and day 15 (2.40 ± 0.09), which was consistent with literature reports.[53] ALP was mainly concentrated on the AP side of the Caco-2 monolayer on day 21. The results revealed that the Caco-2 monolayer appeared distinctly differentiated with polar characteristics.[25]

Bidirectional Transport Assay of 6-MPNs

The apparent permeability coefficient (Papp) value has been reported to be well related to the human absorption data in vivo for many drugs.[54] The Papp value was also used to evaluate the absorption rate of drugs.[55] As shown in Table 1, 6-MPCs gave a Papp (AP-BL) value of 1.952×10^{-6} cm/s, which suggested that the malabsorption of 6-MPCs caused by the low water solubility of 6-MP. It could be seen that the Papp (AP-BL) values of 6-MPNs and 6-MPCs were higher than that of Papp (BL-AP), indicating that 6-MP in the monolayers was mainly transmitted from the AP side to the BL side. Meanwhile, the Papp (AP-BL) value of 6-MPNs was significantly increased compared with 6-MPCs. It has been speculated that 6-MPNs could improve the trafficking of 6-MP from the AP side to the BL side. The efflux rate (ER) of

Table 1 Results of the Bidirectional Transport of 6-MPNs and the Effects of Efflux Inhibitors on the Transport

Samples	Papp (× 10^{-6}) (cm/s)		ER
	AP-BL	BL-AP	
6-MPCs	1.952 ± 0.051*	0.313 ± 0.233	0.154 ± 0.113
6-MPNs	8.494 ± 1.447*	0.196 ± 0.039	0.023 ± 0.004
Indomethacin + 6-MPCs	1.780 ± 0.447	0.308 ± 0.116	0.138 ± 0.042
Indomethacin + 6-MPNs	2.800 ± 0.963*	0.249 ± 0.050	0.112 ± 0.046

Notes: each value represents the mean ± SD (n = 3), * *P* value < 0.05, 6-MPNs vs 6-MPCs or Indomethacin + 6-MPNs vs.6-MPNs.
Abbreviations: Papp, apparent permeability coefficient; ER, efflux ratio; AP-BL, from the AP sides to the BL sides; BL-AP, from the BL sides to the AP sides.

6-MPNs was also lower than that of 6-MPCs, indicating that 6-MPNs may have the ability to reduce the efflux of 6-MP and promote the absorption of 6-MP.[26]

MRP4 is one of the major transporters mediating 6-MP delivery and is distributed in the basolateral side of polarized Caco-2 monolayers expressed in intestinal cells.[56] We found that the Papp (AP-BL) value of 6-MPNs in the presence of indomethacin was significantly lower than that in the absence of indomethacin, indicating that MRP4 inhibitor could inhibit the efflux of 6-MPNs. When 6-MPNs entered the Caco-2 monolayers from AP side, free 6-MP would be partially released from 6-MPNs, and could be excreted from the BL side via MRP4, resulting in the accumulation of the 6-MP on the AP side of the monolayers.[50] Therefore, 6-MP was made into nanoparticles with enhanced transmembrane trafficking capacity and reduced efflux, thereby increasing intestinal absorption.

Effect of 6-MPNs on the Expression of ZO-1

The effect of 6-MPNs on the expression of ZO-1 was investigated by immunofluorescence. We observed that ZO-1 was tightly connected into a network structure in the untreated control group (Figure 4A) and 6-MPCs group (Figure 4B). In contrast, the distribution of ZO-1 in the 6-MPNs group was discontinuous (Figure 4C), and the fluorescence intensity decreased. The results may be due to the electrostatic repulsion between the slightly negative charge 6-MPNs and the negatively charged cell membrane. We inferred that 6-MPNs affected the expression of ZO-1, thereby enhancing intestinal permeability and promoting the paracellular transport.

Additionally, the expression of ZO-1 in Caco-2 monolayers treated with 6-MPNs or 6-MPCs was detected by Western blot. As displayed in Figure 5, the 6-MPCs group had little effect on the expression of ZO-1, while the 6-MPNs group significantly decreased the expression of ZO-1, compared to the control group. Combined with the above immunofluorescence results, 6-MPNs could inhibit the expression of ZO-1, thereby promoting more drugs to enter the cells through

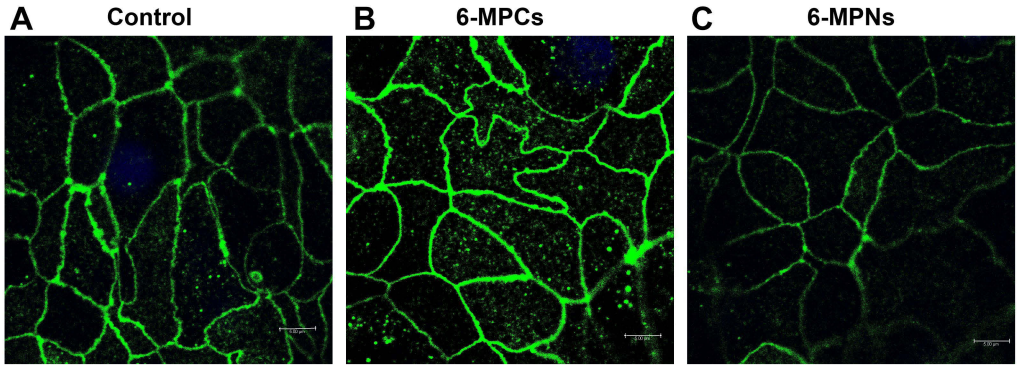

Figure 4 Immunofluorescence images of tight junction protein (ZO-1) in the untreated control group (**A**), 6-MPCs group (**B**) and 6-MPNs group (**C**), respectively (scale bar: 5 μm).

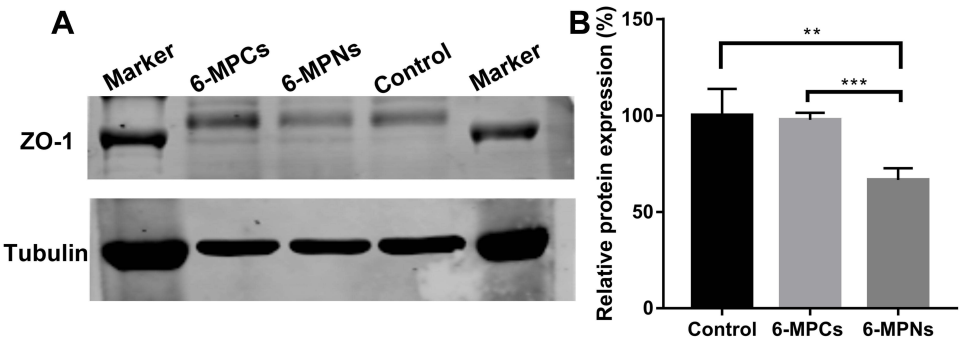

Figure 5 Effects of 6-MPNs on the expression of tight junction protein (ZO-1) in Caco-2 monolayers detected by Western blot. (**A**) Representative immunoblot images (cropped images). (**B**) Quantification analysis of ZO-1 protein expression (**P value < 0.01, ***P value < 0.001).

paracellular transport pathway. The nanomedicines could increase the paracellular permeability in Caco-2 monolayers, concomitantly to tight junction protein ZO-1 redistribution.[27]

Uptake and Trafficking Mechanism in the FAE Monolayers

Assessment of TEER of FAE Monolayers

M cells act as antigen-sampling cells of the intestinal innate immune system, which can constitute the follicle-associated epithelium (FAE) in Peyer's patches (PPs).[57] M cells have good transcytosis capabilities to transmit various materials, such as bacteria, viruses, large molecules and particles from the intestinal lumen to immune cells of the underlying lymphoid tissues.[58] Several studies have reported that an in vitro model of FAE could be obtained by a co-culture of Caco-2 cells and Raji B lymphocytes.[28] The differentiation of M cells in the FAE model was evaluated by measuring the TEER value. As shown in Figure S3, the TEER value of Caco-2 cells and Raji B cells co-cultured for 21 days was 224.41 ± 20.84 $\Omega.cm^2$, which was approximately half of the TEER value of the Caco-2 monolayer. The TEER values of FAE model were significantly reduced, indicating that Caco-2/Raji B co-culture could successfully differentiate M cells.[35]

Uptake Characteristics of 6-MPNs

We examined the uptake mechanism of 6-MPNs in FAE monolayers under different factors of concentrations, times and temperatures. As exhibited in Figure 6A-C, the uptake contents of 6-MP in FAE monolayers increased gradually with increasing concentration, time and temperature. Significantly, the uptake amounts of 6-MPNs were obviously higher than that of 6-MPCs at 100 μM (Figure 6A). Meanwhile, the absorption of 6-MPNs was significantly enhanced compared with 6-MPCs at 0.5 h (Figure 6B). However, the cellular uptake between 6-MPNs and 6-MPCs had no significant difference at 4 h, probably due to the saturation of 6-MP uptake. Figure 6C displays the assimilation of 6-MPNs was better than that of 6-MPCs both at 4°C and 37°C, suggesting that the process might be an energy-consuming active transport.[59] Overall, 6-MPNs promoted the entry of 6-MP into M cells in a time-, concentration- and temperature-dependent manner, but the process of uptake might reach saturation at 4 h. The specific endocytic mechanism of 6-MPNs in M cells would be further studied in the future.

Transport Mechanism of 6-MPNs

In order to assess the transport characteristics of 6-MPNs in FAE monolayers, we investigated the effect of different conditions on the cumulative trafficking content of 6-MP. As exhibited in Figure 6D-F, the content of 6-MP increased with increasing concentration, time and temperature. The cumulative transport content of 6-MPNs was evidently higher than that of 6-MPCs (Figure 6D), especially at the concentrations of 200 μM and 400 μM. The cumulative transport of 6-MPNs also significantly improved compared with 6-MPCs at the time of 0.5 h and 2 h. However, the trafficking of 6-MPNs and 6-MPCs had no significant difference at 4 h (Figure 6E), indicating that the delivery of 6-MP in the FAE monolayers had become saturated. The cumulative transport of 6-MPNs was significantly higher than that of 6-MPCs at both 4°C and 37°C (Figure 6F). The results showed that 6-MPNs enhanced the uptake and transport of 6-MP in M cells. Therefore, 6-MPNs could be absorbed by M cells of Peyer's patches, which improved the passive lymphatic targeting

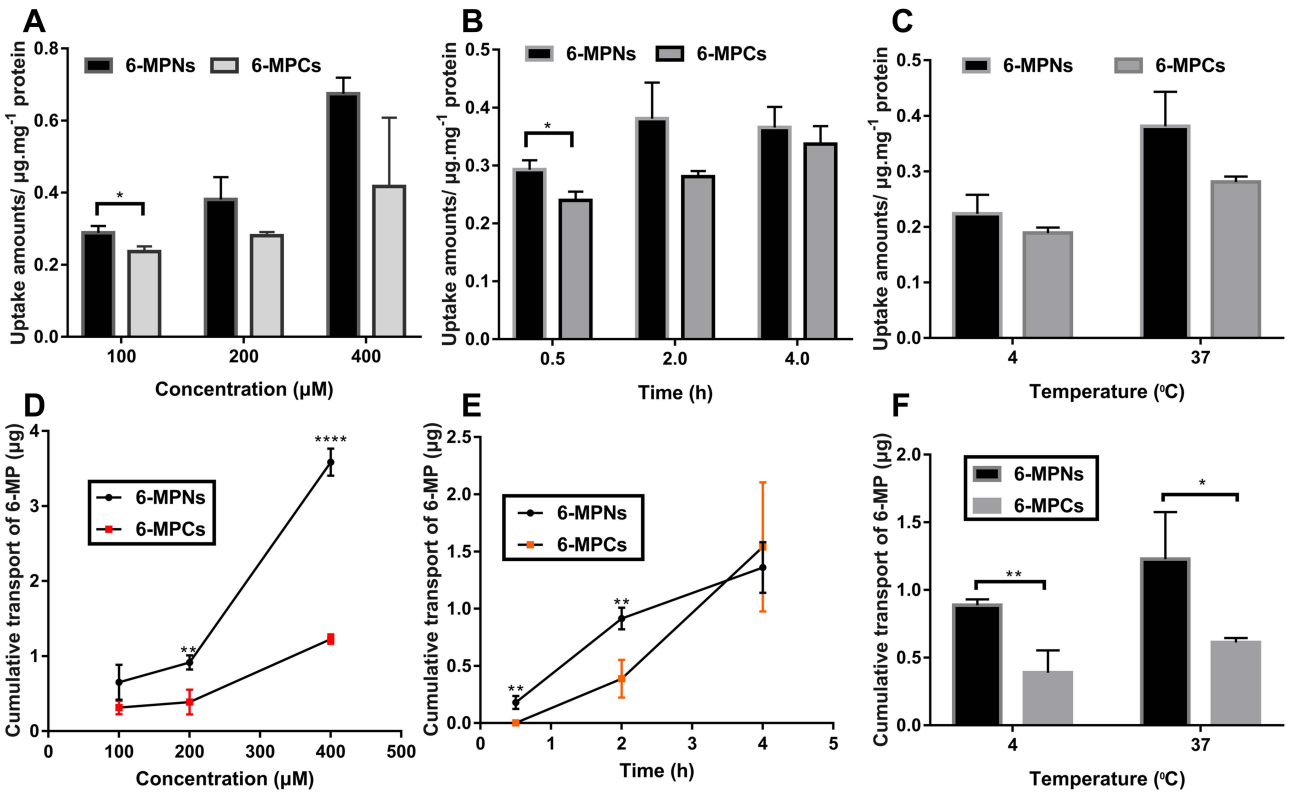

Figure 6 (**A**) Relationship between uptake amounts of 6-MPNs and concentration (*P value < 0.05). (**B**) Relationship between uptake amounts of 6-MPNs and time (*P value < 0.05). (**C**) Relationship between uptake amounts of 6-MPNs and temperature. (**D**) Relationship between cumulative transport of 6-MP and concentration (**P value < 0.01, ****P value < 0.0001). (**E**) Relationship between cumulative transport of 6-MP and time (**P value < 0.01). (**F**) Relationship between cumulative transport of 6-MP and temperature (*P value < 0.05, **P value < 0.01).

and subsequently increased the systemic drug delivery.[9] Additionally, we compared the cumulative transport content of 6-MPNs between the FAE monolayers and Caco-2 monolayers. The results illustrated that the cumulative transport amount of 6-MPNs in FAE monolayers was higher than that in Caco-2 monolayers (see Figure 7A), indicating that M cells significantly enhanced the trafficking of 6-MPNs compared to the intestinal epithelial cells.

Uptake of 6-MPNs in the Peyer's Patches in vivo

We investigated the uptake of 6-MPNs in the PPs of rats to further demonstrate the enhanced absorption of nanomedicines through M cells. Figure 7B presents the concentrations of 6-MP in the PPs and the adjacent small intestinal tissue without the PPs. We discovered that the 6-MP concentration for 6-MPNs (46.2 ± 14.73 μg/mL) in the PPs was

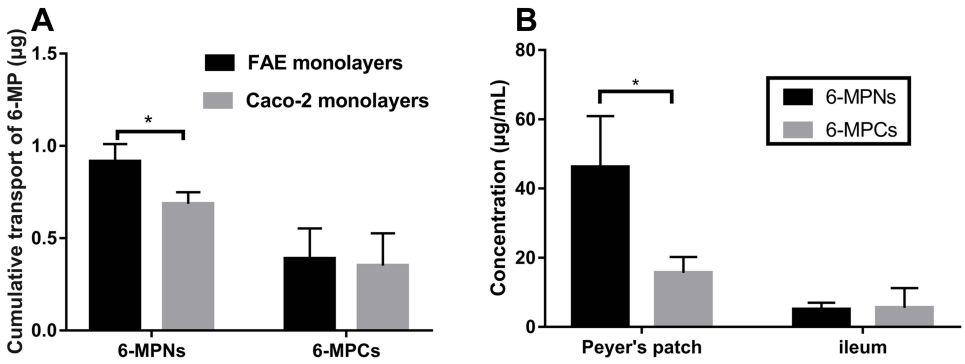

Figure 7 (**A**) The cumulative transport of 6-MP on follicle associated epithelium (FAE) monolayers and Caco-2 monolayers at 2 h, respectively (*P value < 0.05). (**B**) Absorption of 6-MPNs in Peyer's patch and Peyer's patch-free small intestine (*P value < 0.05).

significantly more than the 6-MP concentration for 6-MPCs (5.52 ± 5.73 μg/mL). The results showed that the absorption of 6-MPNs through the PPs significantly increased. Interestingly, the concentrations of 6-MP in the PPs were also higher than that in the adjacent small intestine. Whereas the number and surface area of PPs in the intestinal tract of rats are small, the absorption of 6-MP would be mainly through small intestinal mucosal epithelial cells.

Conclusions

In this study, the superiority of 6-MPNs in cell uptake, transmembrane trafficking and bioavailability improvement was verified. The comprehensive uptake and transport mechanisms of 6-MPNs through Caco-2 cells, polarized Caco-2 monolayers and FAE monolayers were clarified. The uptake of 6-MPNs in Caco-2 cells was a time-, concentration- and energy-dependent pathway. 6-MPNs entered cells through caveolae/lipid raft, caveolin or micropinocytosis mediated endocytosis, which was a nanomedicines-triggered vesicle transport process. The internalized 6-MPNs underwent a vesicle-mediated transmembrane trafficking through the ER-Golgi complex pathway, late endosome-lysosome pathway and microtubule pathway. With the prolonged incubation time, 6-MP would be gradually released from the nanomedicines. Thus, the efflux of 6-MP was significantly inhibited by the inhibitor of MRP4 transporter. The Papp (AP-BL) value of 6-MPNs was increased and the efflux rate of 6-MPNs decreased in Caco-2 monolayers. After the incubation with the inhibitor of MRP4 transporter, the Papp (AP-BL) value of 6-MPNs was significantly reduced. Additionally, 6-MPNs promoted the paracellular transport, thereby increasing the absorption of 6-MP. The uptake and trafficking of 6-MPNs in FAE monolayers were concentration- and energy-dependent, while reaching saturation with time. In vivo, the absorption of 6-MPNs increased by the PPs in the gut, further confirming the superiority of 6-MPNs in enhancing oral bioavailability. Overall, the transmembrane uptake and transport of 6-MPNs are increased in different epithelial cell models and in the gut of rats. These findings may shed light on the oral absorption mechanisms of PLGA nanomedicines.

Acknowledgments

The authors are grateful to the department of pharmacy at Beijing Children's hospital, Children's Hospital of Soochow University, Peking University Third Hospital and the department of pharmaceutical sciences at University of Michigan. This work was supported by Beijing Natural Science Foundation, China (Grant No. L212013, L202048 and L202042), National Natural Science Foundation, China (Grant No. 82173894 and 81903545), Beijing New-star Plan of Science and Technology (Grant No. Z201100006820009).

Disclosure

The authors declare that they have no competing interests in this work.

References

1. Østergaard A, Bohnstedt C, Grell K., et al. Acute lymphoblastic leukemia and down syndrome: 6-mercaptopurine and methotrexate metabolites during maintenance therapy. *Leukemia*. 2021;35(3):863–866. doi:10.1038/s41375-020-0946-2
2. Qiu J, Cheng R, Zhang J, et al. Glutathione-Sensitive Hyaluronic Acid-Mercaptopurine Prodrug Linked via Carbonyl Vinyl Sulfide: a Robust and CD44-Targeted Nanomedicine for Leukemia. *Biomacromolecules*. 2017;18(10):3207–3214. doi:10.1021/acs.biomac.7b00846
3. Gong M, Yang J, Li Y, Gu J. Glutathione-responsive nanoscale MOFs for effective intracellular delivery of the anticancer drug 6-mercaptopurine. *Chem Commun (Camb)*. 2020;56(47):6448–6451. doi:10.1039/D0CC02872J
4. Sierpe R, Noyong M, Simon U, et al. Construction of 6-thioguanine and 6-mercaptopurine carriers based on betacyclodextrins and gold nanoparticles. *Carbohydr Polym*. 2017;177:22–31. doi:10.1016/j.carbpol.2017.08.102
5. Liao J, Peng H, Wei X, et al. A bio-responsive 6-mercaptopurine/doxorubicin based "Click Chemistry" polymeric prodrug for cancer therapy. *Mater Sci Eng C Mater Biol Appl*. 2020;108:110461. doi:10.1016/j.msec.2019.110461
6. Zou Y, Mei D, Yuan J, et al. Preparation, characterization, pharmacokinetic, and therapeutic potential of novel 6-mercaptopurine-loaded oral nanomedicines for acute lymphoblastic leukemia. *Int J Nanomedicine*. 2021;16:1127–1141. doi:10.2147/IJN.S290466
7. Gao L, Liu G, Ma J, et al. Application of drug nanocrystal technologies on oral drug delivery of poorly soluble drugs. *Pharm Res*. 2013;30 (2):307–324. doi:10.1007/s11095-012-0889-z
8. Donahue ND, Acar H, Wilhelm S. Concepts of nanoparticle cellular uptake, intracellular trafficking, and kinetics in nanomedicine. *Adv Drug Deliv Rev*. 2019;143:68–96. doi:10.1016/j.addr.2019.04.008
9. Jia Z, Wignall A, Prestidge C, Thierry B. An ex vivo investigation of the intestinal uptake and translocation of nanoparticles targeted to Peyer's patches microfold cells. *Int J Pharm*. 2021;594:120167. doi:10.1016/j.ijpharm.2020.120167
10. Yu SH, Tang DW, Hsieh HY, et al. Nanoparticle-induced tight-junction opening for the transport of an anti-angiogenic sulfated polysaccharide across Caco-2 cell monolayers. *Acta Biomater*. 2013;9(7):7449–7459. doi:10.1016/j.actbio.2013.04.009

11. Taipalensuu J, Tornblom H, Lindberg G, et al. Correlation of gene expression of ten drug efflux proteins of the ATP-binding cassette transporter family in normal human jejunum and in human intestinal epithelial Caco-2 cell monolayers. *J Pharmacol Exp Ther*. 2001;299(1):164–170. PMID: 11561076.
12. Wang JR, Yu X, Zhou C, et al. Improving the dissolution and bioavailability of 6-mercaptopurine via co-crystallization with isonicotinamide. *Bioorg Med Chem Lett*. 2015;25(5):1036–1039. doi:10.1016/j.bmcl.2015.01.022
13. Wang X, Qiu Y, Wang M, et al. Endocytosis and organelle targeting of nanomedicines in cancer therapy. *Int J Nanomedicine*. 2020;15:9447–9467. doi:10.2147/IJN.S274289
14. Tanaka Y, Manabe A, Fukushima H, et al. Multidrug resistance protein 4 (MRP4) polymorphisms impact the 6-mercaptopurine dose tolerance during maintenance therapy in Japanese childhood acute lymphoblastic leukemia. *Pharmacogenomics J*. 2015;15(4):380–384. doi:10.1038/tpj.2014.74
15. Chen Y, Yuan X, Xiao Z, Jin H, Zhang L, Liu Z. Discovery of novel multidrug resistance protein 4 (MRP4) inhibitors as active agents reducing resistance to anticancer drug 6-Mercaptopurine (6-MP) by structure and ligand-based virtual screening. *PLoS One*. 2018;13(10):e205175. doi:10.1371/journal.pone.0205175
16. Li X, Zhao Z, Li L, Zhou T, Lu W. Pharmacokinetics, in vitro and in vivo correlation, and efficacy of exenatide microspheres in diabetic rats. *Drug Deliv*. 2015;22(1):86–93. doi:10.3109/10717544.2013.871760
17. Hawwa AF, Millership JS, Collier PS, McElnay JC. Development and validation of an HPLC method for the rapid and simultaneous determination of 6-mercaptopurine and four of its metabolites in plasma and red blood cells. *J Pharm Biomed Anal*. 2009;49(2):401–409. doi:10.1016/j.jpba.2008.10.045
18. Kumar GP, Sanganal JS, Phani AR, et al. Anti-cancerous efficacy and pharmacokinetics of 6-mercaptopurine loaded chitosan nanoparticles. *Pharmacol Res*. 2015;100:47–57. doi:10.1016/j.phrs.2015.07.025
19. Mei S, Li X, Gong X, et al. LC-MS/MS analysis of erythrocyte thiopurine nucleotides and their association with genetic variants in patients with neuromyelitis Optica spectrum disorders taking azathioprine. *Ther Drug Monit*. 2017;39(1):5–12. doi:10.1097/FTD.0000000000000362
20. Long L, Lai M, Mao X, et al. Investigation of vitamin B (12)-modified amphiphilic sodium alginate derivatives for enhancing the oral delivery efficacy of peptide drugs. *Int J Nanomedicine*. 2019;14:7743–7758. doi:10.2147/IJN.S218944
21. Leichner C, Jelkmann M, Prüfert F, Laffleur F, Bernkop-Schnürch A. Intestinal enzyme delivery: chitosan/tripolyphosphate nanoparticles providing a targeted release behind the mucus gel barrier. *Eur J Pharm Biopharm*. 2019;144:125–131. doi:10.1016/j.ejpb.2019.09.012
22. Xie Z, Zhang Z, Lv H. Rapamycin loaded TPGS-Lecithins-Zein nanoparticles based on core-shell structure for oral drug administration. *Int J Pharm*. 2019;568:118529. doi:10.1016/j.ijpharm.2019.118529
23. Yang D, Liu D, Deng H, et al. Transferrin functionization elevates transcytosis of nanogranules across epithelium by triggering polarity-associated transport flow and positive cellular feedback loop. *Acs Nano*. 2019;13(5):5058–5076. doi:10.1021/acsnano.8b07231
24. Ming X, Thakker DR. Role of basolateral efflux transporter MRP4 in the intestinal absorption of the antiviral drug Adefovir dipivoxil. *Biochem Pharmacol*. 2010;79(3):455–462. doi:10.1016/j.bcp.2009.08.029
25. Joshi G, Kumar A, Sawant K. Bioavailability enhancement, Caco-2 cells uptake and intestinal transport of orally administered lopinavir-loaded PLGA nanoparticles. *Drug Deliv*. 2016;23(9):3492–3504. doi:10.1080/10717544.2016.1199605
26. Ren S, Liu J, Xue Y, et al. Comparative permeability of three saikosaponins and corresponding saikogenins in Caco-2 model by a validated UHPLC-MS/MS method. *J Pharm Anal*. 2021;11(4):435–443. doi:10.1016/j.jpha.2020.06.006
27. Leve F, Bonfim DP, Fontes G, Morgado-Díaz JA. Gold nanoparticles regulate tight junctions and improve cetuximab effect in colon cancer cells. *Nanomedicine*. 2019;14(12):1565–1578. doi:10.2217/nnm-2019-0023
28. Beloqui A, Brayden DJ, Artursson P, Préat V. A human intestinal M-cell-like model for investigating particle, antigen and microorganism translocation. *Nat Protoc*. 2017;12(7):1387–1399. doi:10.1038/nprot.2017.041
29. Prajapati JB, Verma SD, Patel AA. Oral bioavailability enhancement of agomelatine by loading into nanostructured lipid carriers: peyer's patch targeting approach. *Int J Nanomedicine*. 2018;13:35–38. doi:10.2147/IJN.S124703
30. Wang N, Cheng X, Li N, Wang H, Chen H. Nanocarriers and their loading strategies. *Adv Healthc Mater*. 2019;8(6):e1801002. doi:10.1002/adhm.201801002
31. Jabir M, Sahib UI, Taqi Z, et al. Linalool-loaded glutathione-modified gold nanoparticles conjugated with CALNN peptide as apoptosis inducer and NF-κB translocation inhibitor in SKOV-3 cell line. *Int J Nanomedicine*. 2020;15:9025–9047. doi:10.2147/IJN.S276714
32. Wang W, Fang C, Wang X, et al. Modifying mesoporous silica nanoparticles to avoid the metabolic deactivation of 6-mercaptopurine and methotrexate in combinatorial chemotherapy. *Nanoscale*. 2013;5(14):6249–6253. doi:10.1039/c3nr00227f
33. Albukhaty S, Naderi-Manesh H, Tiraihi T, Sakhi JM. Poly-l-lysine-coated superparamagnetic nanoparticles: a novel method for the transfection of pro-BDNF into neural stem cells. *Artif Cells Nanomed Biotechnol*. 2018;46(sup3):S125–S132. doi:10.1080/21691401.2018.1489272
34. Wright L, Rao S, Thomas N, Boulos RA, Prestidge CA. Ramizol(®) encapsulation into extended release PLGA micro- and nanoparticle systems for subcutaneous and intramuscular administration: in vitro and in vivo evaluation. *Drug Dev Ind Pharm*. 2018;44(9):1451–1457. doi:10.1080/03639045.2018.1459676
35. Yin Y, Deng H, Wu K, et al. A multiaspect study on transcytosis mechanism of sorafenib nanogranules engineered by high-gravity antisolvent precipitation. *J Control Release*. 2020;323:600–612. doi:10.1016/j.jconrel.2020.04.008
36. Deng F, Zhang H, Wang X, et al. Transmembrane pathways and mechanisms of rod-like paclitaxel nanocrystals through MDCK polarized monolayer. *ACS Appl Mater Interfaces*. 2017;9(7):5803–5816. doi:10.1021/acsami.6b15151
37. Macia E, Ehrlich M, Massol R, Boucrot E, Brunner C, Kirchhausen T. Dynasore, a cell-permeable inhibitor of dynamin. *Dev Cell*. 2006;10(6):839–850. doi:10.1016/j.devcel.2006.04.002
38. Kadlecova Z, Spielman SJ, Loerke D, Mohanakrishnan A, Reed DK, Schmid SL. Regulation of clathrin-mediated endocytosis by hierarchical allosteric activation of AP2. *J Cell Biol*. 2017;216(1):167–179. doi:10.1083/jcb.201608071
39. Song X, Li R, Deng H, et al. Receptor mediated transcytosis in biological barrier: the influence of receptor character and their ligand density on the transmembrane pathway of active-targeting nanocarriers. *Biomaterials*. 2018;180:78–90. doi:10.1016/j.biomaterials.2018.07.006
40. Palomba R, Palange AL, Rizzuti IF, et al. Modulating Phagocytic Cell Sequestration by Tailoring Nanoconstruct Softness. *Acs Nano*. 2018;12(2):1433–1444. doi:10.1021/acsnano.7b07797

41. Xiao GS, Zhang YH, Wu W, Sun HY, Wang Y, Li GR. Genistein and tyrphostin AG556 decrease ultra-rapidly activating delayed rectifier K (+) current of human atria by inhibiting EGF receptor tyrosine kinase. *Br J Pharmacol*. 2017;174(6):454–467. doi:10.1111/bph.13710
42. Atale SS, Dyawanapelly S, Jagtap DD, Jain R, Dandekar P. Understanding the nano-bio interactions using real-time surface plasmon resonance tool. *Int J Biol Macromol*. 2019;123:97–107. doi:10.1016/j.ijbiomac.2018.11.039
43. Nickel W. Pathways of unconventional protein secretion. *Curr Opin Biotechnol*. 2010;21(5):621–626. doi:10.1016/j.copbio.2010.06.004
44. Yoon S, Rossi JJ. Aptamers: uptake mechanisms and intracellular applications. *Adv Drug Deliv Rev*. 2018;134:22–35. doi:10.1016/j.addr.2018.07.003
45. Mauvezin C, Nagy P, Juhász G, Neufeld TP. Autophagosome-lysosome fusion is independent of V-ATPase-mediated acidification. *Nat Commun*. 2015;6:7007. doi:10.1038/ncomms8007
46. Xu Z, Schaedel L, Portran D, et al. Microtubules acquire resistance from mechanical breakage through intralumenal acetylation. *Science*. 2017;356(6335):328–332. doi:10.1126/science.aai8764
47. Thietart S, Rautou PE. Extracellular vesicles as biomarkers in liver diseases: a clinician's point of view. *J Hepatol*. 2020;73(6):1507–1525. doi:10.1016/j.jhep.2020.07.014
48. Reid G, Wielinga P, Zelcer N, et al. Characterization of the transport of nucleoside analog drugs by the human multidrug resistance proteins MRP4 and MRP5. *Mol Pharmacol*. 2003;63(5):1094–1103. doi:10.1124/mol.63.5.1094
49. Maher JM, Slitt AL, Cherrington NJ, Cheng X, Klaassen CD. Tissue distribution and hepatic and renal ontogeny of the multidrug resistance-associated protein (Mrp) family in mice. *Drug Metab Dispos*. 2005;33(7):947–955. doi:10.1124/dmd.105.003780
50. Ming X, Thakker DR. Role of basolateral efflux transporter MRP4 in the intestinal absorption of the antiviral drug Adefovir dipivoxil. *Biochem Pharmacol*. 2010;79(3):455–462. doi:10.1016/j.bcp.2009.08.029
51. Yaneff A, Sahores A, Gómez N, Carozzo A, Shayo C, Davio C. MRP4/ABCC4 As a New Therapeutic Target: meta-Analysis to Determine cAMP Binding Sites as a Tool for Drug Design. *Curr Med Chem*. 2019;26(7):1270–1307. doi:10.2174/0929867325666171229133259
52. Calhau C, Martel F, Hipólito-Reis C, Azevedo I. Modulation of uptake of organic cationic drugs in cultured human colon adenocarcinoma Caco-2 cells by an ecto-alkaline phosphatase activity. *J Cell Biochem*. 2002;87(4):408–416. doi:10.1002/jcb.10306
53. Abramov VM, Kosarev IV, Priputnevich TV, et al. S-layer protein 2 of vaginal Lactobacillus crispatus 2029 enhances growth, differentiation, VEGF production and barrier functions in intestinal epithelial cell line Caco-2. *Int J Biol Macromol*. 2021;189:410–419. doi:10.1016/j.ijbiomac.2021.08.150
54. Yee S. In vitro permeability across Caco-2 cells (colonic) can predict in vivo (small intestinal) absorption in man--fact or myth. *Pharm Res*. 1997;14(6):763–766. doi:10.1023/A:1012102522787
55. Wang Y, Bai X, Hu B, et al. Transport mechanisms of polymannuronic acid and polyguluronic acid across Caco-2 cell monolayers. *Pharmaceutics*. 2020;12(2). doi:10.3390/pharmaceutics12020167.
56. Furmanski BD, Hu S, Fujita KI, et al. Contribution of ABCC4-mediated gastric transport to the absorption and efficacy of dasatinib. *Clin Cancer Res*. 2013;19(16):4359–4370. doi:10.1158/1078-0432.CCR-13-0980
57. Beloqui A, Brayden DJ, Artursson P, Préat V. A human intestinal M-cell-like model for investigating particle, antigen and microorganism translocation. *Nat Protoc*. 2017;12(7):1387–1399. doi:10.1038/nprot.2017.041
58. Brun E, Barreau F, Veronesi G, et al. Titanium dioxide nanoparticle impact and translocation through ex vivo, in vivo and in vitro gut epithelia. *Part Fibre Toxicol*. 2014;11:13. doi:10.1186/1743-8977-11-13
59. Des Rieux A, Fievez V, Théate I, Mast J, Préat V, Schneider Y-J. An improved in vitro model of human intestinal follicle-associated epithelium to study nanoparticle transport by M cells. *Eur J Pharm Sci*. 2007;30(5):380–391. doi:10.1016/j.ejps.2006.12.006